

Hadronic parity violation in $\vec{n}p \rightarrow d\gamma$ with effective field theory

C. H. Hyun,^{1,*} S. Ando,^{1,†} and B. Desplanques^{2,‡}

¹*Department of Physics and Institute of Basic Science,*

Sungkyunkwan University, Suwon 440-746, Korea

²*LPSC, Université Joseph Fourier Grenoble 1, CNRS/IN2P3,*

Institut National Polytechnique de Grenoble, F-38026 Grenoble Cedex, France

(Dated: May 31, 2007)

Abstract

The parity-violating nucleon-nucleon (NN) potential is considered up to next-to-next-to leading order in heavy-baryon chiral perturbation theory. We include one-pion exchange at leading order and the two-pion exchange and two-nucleon contact terms at next-to-next-to-leading order. The effects of intermediate (two-pion exchange) and short-range (two-nucleon contact) terms are probed by calculating the photon asymmetry A_γ in $\vec{n}p \rightarrow d\gamma$ employing Siegert's theorem and an accurate phenomenological potential for the parity-conserving NN interaction. We explore in detail the uncertainties due to the parameters that control the contribution of the short-range interaction. We obtain about 20% uncertainty in the value of A_γ up to the next-to-next-to leading order. We discuss the implication of this uncertainty for the determination of the weak pion-nucleon coupling constant and how the uncertainty can be reduced.

PACS numbers: 21.30.Fe, 12.15.Ji

*Electronic address: hch@meson.skku.ac.kr

†Electronic address: sando@meson.skku.ac.kr

‡Electronic address: desplanq@lpsc.in2p3.fr

I. INTRODUCTION

The perturbative calculation of the strong nucleon-nucleon (NN) potential in the framework of effective-field theory (EFT) was first suggested by Weinberg [1]. Counting rules systematically arrange the magnitude of a two-nucleon irreducible diagram for calculating the NN potential in terms of Q/Λ_χ where Q denotes a typical small momentum and/or pion mass m_π and Λ_χ the chiral scale. Accordingly, one-pion exchange (OPE) and a constant two-nucleon contact term are the most dominant contributions. At the next-to-next-to-leading order (NNLO), there are two-pion exchange (TPE), contact terms with two derivatives and/or pion mass factors, relativistic corrections, *etc.* If one goes to higher orders, there appear multi-pion exchanges and contact terms with more than two derivatives and/or m_π , and heavy-meson exchange possibly comes into play. At low energies where EFT is applicable, a physical process is mostly governed by the long-range interaction and it is more or less insensitive to what's happening in the short-range region. Thus in most cases, heavy mesons are integrated out from the Lagrangian and their short-range interaction is accounted for by contact terms. A physical observable calculated with the NN potential must be independent of a cutoff value that is introduced in calculating loop diagrams and its transformation to coordinate space. This can be achieved by contact terms together with some renormalization method. Strong EFT potentials thus obtained were applied to the analysis of NN scattering phase shifts [2, 3, 4], showing a well-behaved convergence and predictive power. The role of the NNLO potential was intensively explored in [5] where it was shown to be important in extending the predictability of the EFT to higher energies. In addition, it gives a correction to the leading order (LO) potential which is non-negligible even at the energy of a few MeV.

The above approach has recently been extended to the parity-violating (PV) nucleon-nucleon (NN) potential [6]. Since then, it has been used for the calculation of observables [7, 8], especially the PV photon asymmetry A_γ in $\vec{n}p \rightarrow d\gamma$ at threshold, where it could be of some relevance.

The PV NN potential is obtained by replacing a parity-conserving (PC) vertex in the strong NN potential with a PV vertex. Most of the low-energy PV calculations have relied on a one-meson-exchange potential with DDH estimates for the PV meson-nucleon coupling constants [9]. Theoretical estimations of A_γ have been extensively worked out with this model (see Refs. [10, 11, 12, 13, 14] for recent ones). The most elaborate results with

various strong-interaction models [11, 12, 13, 14] turn out to be basically identical. The asymmetry is dominated by the PV one-pion-exchange potential (OPEP) and the heavy-meson contribution is negligible. One can thus discuss whether the measurements of A_γ could provide us with an opportunity to determine the weak pion-nucleon coupling constant h_π^1 . Some literature has also investigated the PV two-pion-exchange potential (TPEP) [15, 16, 17]. Its contribution to A_γ , calculated with the Hamada-Johnston potential, amounts to about -7% of the OPEP contribution [18]. Not surprisingly, the TPEP is also part of the pionful EFT approach where it appears at NNLO [6]. In the present work, we concentrate on its contribution to the asymmetry A_γ mentioned above and consider the questions that its estimate raises.

Since the PV asymmetry in $\vec{n}p \rightarrow d\gamma$ is sensitive to the one-pion-exchange contribution, we adopt the heavy-baryon chiral perturbation (HB χ PT). We employ the Argonne v18 potential for the PC potential and the Siegert's theorem for the current operators and consider the PV potential relevant to $\vec{n}p \rightarrow d\gamma$ up to NNLO. This calculation will allow us to estimate the order and the magnitude of higher-order corrections, which will be important in pinning down the value of h_π^1 and its uncertainty. At the same time, it will provide a criterion for the validity of the EFT approach to the PV phenomena.

II. FORMALISM

In HB χ PT, the order of a diagram is counted in terms of a small momentum Q (more precisely Q/Λ_χ) with the following rules; i) a meson propagator is counted as Q^{-2} , ii) a nucleon propagator as Q^{-1} , iii) a loop integral as Q^4 , iv) a vertex as Q^d where d is the number of derivatives at the given vertex. With these counting rules, diagrams in Fig. 1 constitute the contributions up to NNLO. One-pion exchange (a), and the two-pion exchange (b-d) and the contact (CT) (e) terms respectively represent LO and NNLO contributions.

The PV potential is odd in powers of the momentum transfer in momentum space or the radial vector in the configuration space, which changes the orbital angular state by an odd number. In order to keep the wave function of a fermion system antisymmetric, the PV potential must satisfy the condition $\Delta(L + S + T) = \text{even}$, where L , S and T denote orbital, spin and isospin states, respectively. The change of $S + T$ in the PV potential should be an odd number. For a two-fermion system, the possible combinations of the spin and

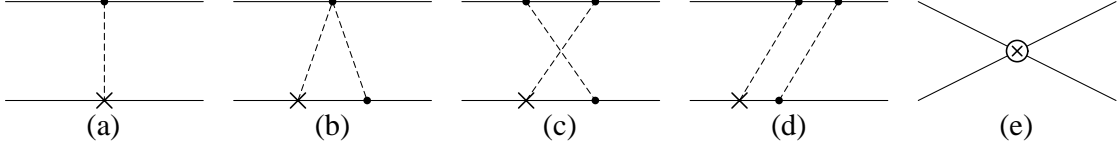


FIG. 1: Diagrams for PV NN potential up to NNLO: (a) for LO ($\mathcal{O}(Q^{-1})$) OPE, and (b-e) for NNLO ($\mathcal{O}(Q^1)$) TPE + CT. Lines (dashed lines) denote nucleons (pions), vertices with a dot represent PC vertices, vertices with “ \times ” represent the PV vertex proportional to h_π^1 , and a vertex with “ \otimes ” denotes the NN contact vertex function proportional to the coefficient C_6^R .

isospin operators in the PV potential must thus be $(\Delta S, \Delta T) = (1, 0)$ or $(0, 1)$. Among various possible combinations of spin and isospin operators that give $\Delta(S + T) = 1$, the term relevant to our estimation of A_γ has the following form in momentum space

$$\tilde{V}_i(\mathbf{q}) = i(\boldsymbol{\tau}_1 \times \boldsymbol{\tau}_2)^z (\boldsymbol{\sigma}_1 + \boldsymbol{\sigma}_2) \cdot \mathbf{q} \tilde{v}_i(q), \quad (1)$$

with $q \equiv |\mathbf{q}|$ and $\mathbf{q} = \mathbf{p}_1 - \mathbf{p}'_1$, where \mathbf{p}_1 (\mathbf{p}'_1) is the momentum of a nucleon 1 in the initial (final) state. The OPE, TPE and CT terms are obtained as

$$\tilde{v}_{1\pi}(q) = -\frac{g_A h_\pi^1}{2\sqrt{2}f_\pi} \frac{1}{q^2 + m_\pi^2}, \quad (2)$$

$$\tilde{v}_{2\pi}(q) = \sqrt{2}\pi \frac{h_\pi^1}{\Lambda_\chi^3} \left\{ g_A \tilde{L}(q) - g_A^3 [3\tilde{L}(q) - \tilde{H}(q)] \right\}, \quad (3)$$

$$\tilde{v}_{\text{CT}} = C_6^R, \quad (4)$$

with

$$\tilde{L}(q) = \frac{\sqrt{q^2 + 4m_\pi^2}}{q} \ln \left(\frac{\sqrt{q^2 + 4m_\pi^2} + q}{2m_\pi} \right), \quad (5)$$

$$\tilde{H}(q) = \frac{4m_\pi^2}{q^2 + 4m_\pi^2} \tilde{L}(q), \quad (6)$$

where g_A is the axial coupling constant, f_π the pion-decay constant and $\Lambda_\chi = 4\pi f_\pi$. The constant C_6^R is the renormalized LEC for a NN contact term C_6 in [6]. It subsumes the role of all the heavy degrees of freedom integrated out from the theory. We will discuss how to treat the renormalized LEC in our investigation after giving the formulae for the potentials in configuration space.

The potential in Eq. (1) transformed to configuration space takes the form

$$V_i(\mathbf{r}) = \int \frac{d^3\mathbf{q}}{(2\pi)^3} \tilde{V}_i(\mathbf{q}) e^{-i\mathbf{q}\cdot\mathbf{r}}$$

$$= i(\boldsymbol{\tau}_1 \times \boldsymbol{\tau}_2)^z (\boldsymbol{\sigma}_1 + \boldsymbol{\sigma}_2) \cdot [\mathbf{p}, v_i(r)], \quad (7)$$

where \mathbf{p} is the conjugate momentum of the relative coordinate $\mathbf{r} \equiv \mathbf{r}_1 - \mathbf{r}_2$. For an easier numerical calculation, we rewrite Eqs. (5, 6) in the dispersion-relation form as

$$\tilde{L}(q) = - \int_{4m_\pi^2}^{\infty} \frac{dt'}{2\sqrt{t'}} \sqrt{t' - 4m_\pi^2} \left(\frac{1}{t' + q^2} - \frac{1}{t' - 4m_\pi^2} \right), \quad (8)$$

$$\tilde{H}(q) = \frac{4m_\pi^2}{2} \int_{4m_\pi^2}^{\infty} \frac{dt'}{\sqrt{t'}} \frac{1}{\sqrt{t' - 4m_\pi^2}} \frac{1}{t' + q^2}. \quad (9)$$

In calculating the Fourier transformation of Eq. (1), in order to obtain a convergent, analytical result, we introduce monopole form factors of the type $(\Lambda^2 - m_\pi^2)/(\Lambda^2 + q^2)$ in Eq. (2) and $\Lambda^2/(\Lambda^2 + q^2)$ in Eqs. (3, 4). This particular choice for the OPEP preserves the long-range part, which, otherwise, could not be easily corrected for with contact interactions. The roles of the form factor and the cutoff are (i) to make the numerical calculation easier and more efficient, and (ii) to cut away the high-momentum region where the dynamics is essentially unknown and whose detail is irrelevant to low-energy processes. We emphasize that the cutoff is arbitrary for a part and that final results should not depend on its value. With the form factor, we rewrite the potential in configuration space as

$$V_i^\Lambda(\mathbf{r}) = i(\boldsymbol{\tau}_1 \times \boldsymbol{\tau}_2)^z (\boldsymbol{\sigma}_1 + \boldsymbol{\sigma}_2) \cdot [\mathbf{p}, v_i^\Lambda(r)], \quad (10)$$

where

$$v_{1\pi}^\Lambda(r) = \frac{g_A h_\pi^1}{2\sqrt{2}f_\pi} \frac{1}{4\pi r} (e^{-m_\pi r} - e^{-\Lambda r}), \quad (11)$$

$$v_{2\pi}^\Lambda(r) = \sqrt{2}\pi \frac{h_\pi^1}{\Lambda_\chi^3} \left\{ g_A L^\Lambda(r) - g_A^3 [3L^\Lambda(r) - H^\Lambda(r)] \right\}, \quad (12)$$

$$v_{\text{CT}}^\Lambda(r) = -C_6^R \Lambda^2 \frac{e^{-\Lambda r}}{4\pi r}, \quad (13)$$

with

$$L^\Lambda(r) = \frac{\Lambda^2}{8\pi r} \int_{4m_\pi^2}^{\infty} \frac{dt'}{\sqrt{t'}} \sqrt{t' - 4m_\pi^2} \left(\frac{e^{-\sqrt{t'}r} - e^{-\Lambda r}}{\Lambda^2 - t'} - \frac{e^{-\Lambda r}}{t' - 4m_\pi^2} \right), \quad (14)$$

$$H^\Lambda(r) = -\frac{m_\pi^2 \Lambda^2}{2\pi r} \int_{4m_\pi^2}^{\infty} \frac{dt'}{\sqrt{t'}} \frac{1}{\sqrt{t' - 4m_\pi^2}} \frac{e^{-\sqrt{t'}r} - e^{-\Lambda r}}{\Lambda^2 - t'}. \quad (15)$$

Notice that in the $\Lambda \rightarrow \infty$ limit, $L^\Lambda(r)$ is proportional to the difference of two singular terms, r^{-3} and $\delta(\vec{r})$ with an infinite coefficient. The 3-dimensional integral over \vec{r} is however finite and has the sign of the contact term.

The form of C_6^R depends on the regularization scheme. In Ref. [6], all the constant terms obtained from the dimensional regularization ($d = 4 - 2\epsilon$) of TPE diagrams are included in C_6^R , leading to

$$C_6^R(\text{MX}) = C_6 - h_\pi^1 \frac{\pi g_A}{\sqrt{2} \Lambda_\chi^3} (1 - 3g_A^2) \left[\frac{1}{\epsilon} - \gamma + \ln(4\pi) + 2 \ln \left(\frac{\mu}{m_\pi} \right) + 2 \right], \quad (16)$$

where the abbreviation MX stands for ‘maximal subtraction’, $\gamma = 0.5772$ and μ is the renormalization scale. In the minimal subtraction (MN) scheme, the renormalized LEC satisfies the relation

$$C_6^R(\text{MX}) = C_6^R(\text{MN}) + C_{\text{mn}}, \quad (17)$$

where

$$C_{\text{mn}} = -h_\pi^1 \frac{\sqrt{2} \pi g_A}{\Lambda_\chi^3} (1 - 3g_A^2) \left[\ln \left(\frac{\mu}{m_\pi} \right) + 1 \right]. \quad (18)$$

Either $C_6^R(\text{MX})$ or $C_6^R(\text{MN})$ has to be determined from a calculation using the underlying theory or from experimental data with good statistics, neither of which is available at present. We can only consider possible contributions to C_6^R , leaving for the future the theoretical or experimental determination of the remaining part.

A first contribution is suggested by the one-meson exchange model. In the heavy-meson limit, the leading order of the ρ -meson propagator is a constant and the corresponding term can be regarded as part of C_6^R . It reads

$$C_6^R(\rho) = \frac{g_{\rho NN} h_\rho^{1'}}{2m_N m_\rho^2}, \quad (19)$$

where $h_\rho^{1'}$ is the PV ρNN coupling constant in the potential. A non-vanishing value is obtained for this coupling in a soliton model, $h_\rho^{1'} = -2.2 \times 10^{-7}$ [19]. Leaving aside consistency problems between different approaches, double counting with the TPEP considered here for instance, we notice that it compares to the DDH best value of h_π^1 ($= 4.6 \times 10^{-7}$). The corresponding value of $C_6^R(\rho)$ is $-1.20 \times 10^{-9} \text{ MeV}^{-3}$ in units of this value of h_π^1 .

A second contribution is provided by the MN scheme where C_{mn} is treated independently of $C_6^R(\text{MN})$, which consequently gives μ dependence in the result. If we choose $\mu = m_\rho$, we have $C_{\text{mn}} = 4.174 \times 10^{-8} \text{ MeV}^{-3}$ in units of h_π^1 . This value is one order larger than $C_6^R(\rho)$, and therefore the effect of C_{mn} and the dependence on μ can be non-negligible.

A third contribution stems from a deeper examination of the TPEP. This one has been obtained by removing from the square-box diagram the iterated OPEP, ignoring the cutoff

introduced in actual calculations. The correction, which involves the whole strong interaction and should contribute to make the results cutoff independent, is not easy to calculate. This last property can however be restored with a minimal contribution which cancels the cutoff-dependent term in Eq. (11). This one corresponds to

$$C_6^R(\pi, \Lambda) = -\frac{g_A h_\pi^1}{2\sqrt{2}f_\pi\Lambda^2}. \quad (20)$$

Its value compares to the C_{mn} one for the smallest values of the cutoff Λ considered here.

We will explore the above contributions in detail in the analysis of the photon asymmetry in $\vec{n}p \rightarrow d\gamma$, A_γ . This quantity is defined from the differential cross section of the process as

$$\frac{d\sigma}{d\Omega} \propto 1 + A_\gamma \cos \theta, \quad (21)$$

where θ is the angle between the neutron polarization and the out-going photon momentum. Non-zero A_γ values arise from the interference of opposite-parity transition amplitudes, *e.g.* M1 and E1. At the thermal energy where the process occurs, lowest order EM operators may suffice, therefore we consider the E1 operator,

$$\mathbf{J}_{\text{E1}} = -i\frac{\omega_\gamma}{4} (\tau_1^z - \tau_2^z) \mathbf{r}, \quad (22)$$

where ω_γ is the out-going-photon energy. At the leading order of h_π^1 , A_γ is proportional to h_π^1 , and we can write A_γ as

$$A_\gamma = a_\gamma h_\pi^1, \quad (23)$$

with

$$a_\gamma = -2\frac{\text{Re}(\mathcal{M}_1\mathcal{E}_1^*)}{|\mathcal{M}_1|^2}, \quad (24)$$

where \mathcal{E}_1 and \mathcal{M}_1 are matrix elements of the E1 and M1 transitions, respectively. Analytic forms of these amplitudes can be found in [14].

III. RESULTS AND DISCUSSION

Here we present and discuss numerical results corresponding to the various contributions outlined in the previous section. The OPE and TPE potentials in configuration space are considered as well as individual and total contributions to the A_γ asymmetry.

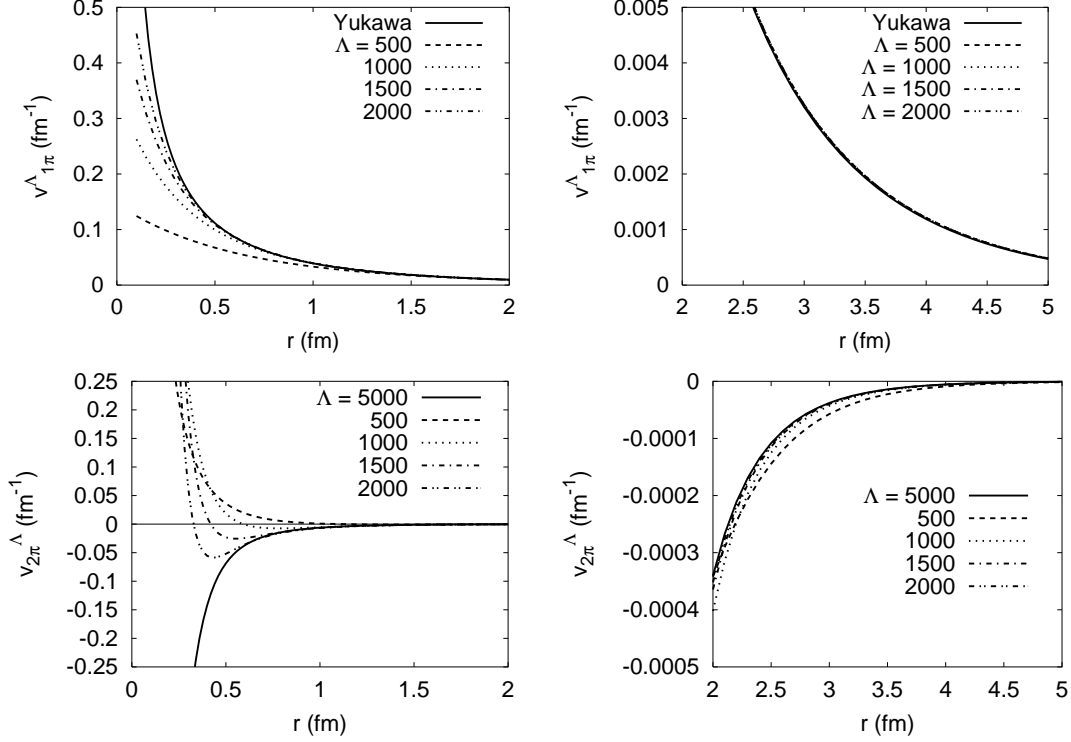


FIG. 2: Potentials $v_{1\pi}^\Lambda(r)$ (upper row) and $v_{2\pi}^\Lambda(r)$ (lower row) divided by h_π^1 in the short-intermediate (left column) and long (right column) ranges. In the figures for TPEP, the result for $\Lambda = 5000$ MeV is shown as an example of the limiting case $\Lambda \rightarrow \infty$.

The OPEP term $v_{1\pi}^\Lambda(r)$ is shown in the top rows of Fig. 2 in the short (left) and long (right) ranges separately. The curve denoted by ‘Yukawa’ corresponds to the infinite-cutoff value. Increasing the cutoff Λ , the potential converges to the Yukawa one. While the potential is almost independent of the cutoff value in the range $r > 1$ fm, some sizable deviation from the Yukawa form occurs at $r < 1$ fm when the cutoff is equal to 500 MeV.

The TPEP term $v_{2\pi}^\Lambda(r)$ is in the bottom row of Fig. 2. The long-range behavior is, as OPEP, independent of the cutoff value, but its magnitude is smaller by an order of magnitude. Therefore one can conclude that the long-range dynamics is essentially cutoff independent and governed by OPEP. On the contrary, TPEP changes sign in the intermediate or short range (bottom-left panel), and the position at which the sign change occurs depends on the cutoff value. What matters in this behavior is that this change occurs in the intermediate region where TPEP is supposed to play an important role. The effect of this strong cutoff dependence is investigated below for the physical observable of interest here.

Λ (MeV)	500	1000	1500	2000
a_γ^{OPE}	-0.0992	-0.1104	-0.1117	-0.1119
a_γ^{TPE}	-0.0022	0.0073	0.0117	0.0133
$a_\gamma^{\text{LEC}}(\rho)$	-0.0008	-0.0004	-0.0002	-0.0001
$a_\gamma^{\text{LEC}}(\text{mn})$	0.0264	0.0134	0.0065	0.0036
$a_\gamma^{\text{LEC}}(\pi, \Lambda)$	-0.0128	-0.0016	-0.0004	-0.0001

TABLE I: Contribution to the asymmetry from each term as a function of the cutoff Λ . The renormalization scale is chosen as $\mu = m_\rho$ in the minimal subtraction LEC contribution ($\propto C_{\text{mn}}$).

Table I shows the contribution of each term to the coefficient a_γ entering the expression of the asymmetry A_γ , Eq. (23). The OPEP contribution with $\Lambda = 500$ MeV is slightly smaller in magnitude than those with the other cutoff values, but the result as a whole is independent of the cutoff value. The small dependence of a_γ^{OPE} on the cutoff Λ can be attributed to the sensitivity of $v_{1\pi}^\Lambda(r)$ in the range $r < 1$ fm to Λ . On the other hand, it seems that the region below $r \sim 0.5$ fm gives an almost negligible contribution since $v_{1\pi}^\Lambda(r)$ with $\Lambda = 1000$ MeV differs sizably from its value with larger cutoff values below $r \sim 0.5$ fm, but the difference in a_γ^{OPE} is negligible. Roughly speaking, the significant contribution to a_γ comes from the region $r \gtrsim 0.5$ fm.

The TPEP contribution to a_γ , on the other hand, varies significantly in sign and magnitude. The change of a_γ^{TPE} can be attributed to the strong dependence of $v_{2\pi}^\Lambda(r)$ on the cutoff value in the intermediate and short ranges. The sign change, which can be ascribed to a contact term implied by the method used to calculate the potential, is physically questionable. From the behavior of $v_{1\pi}^\Lambda(r)$ and the sign of a_γ^{OPE} , one can deduce that a decreasing term gives a negative contribution to a_γ . With a smaller cutoff value, the decreasing part of TPEP spreads to a larger r . For instance, TPEP becomes increasing at around $r = 0.4$ fm for $\Lambda = 2000$ MeV, but this occurs around 1.5 fm for $\Lambda = 500$ MeV. In the discussion of a_γ^{OPE} , we argued that most of the contribution arises from the region $r \gtrsim 0.5$ fm. With a smaller cutoff value, the negative contribution to a_γ^{TPE} becomes more substantial and, as a result, a_γ^{TPE} with $\Lambda = 500$ MeV is negative. The convergence of the TPE contribution with an increasing cutoff value is slower than the OPE one, which can also be attributed to the

Λ (MeV)		500	1000	1500	2000
$a_\gamma^{\text{tot}}(\text{MX})$		-0.1149	-0.1051	-0.1006	-0.0988
	$\mu = 2m_\pi$	-0.0987	-0.0969	-0.0966	-0.0966
$a_\gamma^{\text{tot}}(\text{MN})$	$\mu = m_\rho$	-0.0885	-0.0917	-0.0941	-0.0952
	$\mu = 1 \text{ GeV}$	-0.0859	-0.0904	-0.0935	-0.0949

TABLE II: Total sum of OPE, TPE and LEC contributions in the MX and MN schemes. Each row of $a_\gamma^{\text{tot}}(\text{MN})$ corresponds to $\mu = 2m_\pi$, m_ρ and 1000 MeV from the top, respectively.

strong dependence of TPEP on the cutoff value. However, a_γ^{TPE} will not increase indefinitely and we guess that a_γ^{TPE} with $\Lambda = 2000$ MeV will not be much different from that in the limiting case $\Lambda \rightarrow \infty$. For example, $a_\gamma^{\text{TPE}} = 0.0146$ with $\Lambda = 5000$ MeV, which suggests that the rate of increase with respect to Λ has decreased compared to that in the smaller Λ region. Thus, without significant error, we can conclude that the TPE contribution to a_γ is about 10% of the OPE.

All the LEC contributions ($\propto C_6^R(\rho)$, C_{mn} and $C_6^R(\pi, \Lambda)$) have a magnitude that decreases with increasing cutoff value. With a smaller cutoff value, $v_{\text{CT}}^\Lambda(r)$ is less short-range peaked and more spread out to larger r . Taking into account the $r \gtrsim 0.5$ fm criterion, it is a natural result to have a a_γ^{LEC} smaller in magnitude with a larger cutoff. The $C_6^R(\rho)$ contribution is small in comparison of the other ones, but this could be a result of the particular value of $h_\rho^{1'}$ used in its calculation [19]. The contribution of the C_{mn} term, absent in the MX scheme, is comparable to the TPEP one. Consequently, the choice of the regularization scheme can give a non-trivial effect for the total sum of OPE, TPE and LEC contributions, a_γ^{tot} . The $C_6^R(\pi, \Lambda)$ contribution is also comparable to the TPEP one, but only at small Λ . As expected from its derivation, it removes the Λ dependence of the OPE contribution.

In Table II, we show the sum of OPE, TPE and LEC contributions to a_γ , for the MX and MN regularization schemes. Comparison of the results in different columns gives insight on the cutoff dependence, while comparison of rows in the MN case shows how results vary with the renormalization scale, μ . This scale is conventionally set to the ρ -meson mass, the chiral symmetry breaking scale Λ_χ or the order of the cutoff value Λ [4]. Exploring the corresponding dependence with values $\mu = 2m_\pi$, m_ρ and 1000 MeV, a_γ^{tot} is found to increase with μ (algebraically). This is simply related to the contribution of the C_{mn} term

which is a logarithmically increasing function of that variable. The dependence on the cutoff value is found to be opposite in the MX scheme and the MN one with $\mu = m_\rho$. Since the contributions of the OPE plus $C_6^R(\pi, \Lambda)$ and $C_6^R(\rho)$ terms remain almost constant, the Λ dependence in the MX scheme is mainly due to the TPE one. The opposite effect in the MN scheme results from the further LEC contribution involving C_{mn} , which roughly has the same magnitude but is decreasing instead of increasing with Λ . The overall Λ dependence is sensitive to the μ value and can almost vanish ($\mu = 2m_\pi$) as well as be more pronounced ($\mu = 1000$ MeV).

Because of the considerable dependence on the cutoff Λ (MX scheme) or on both the cutoff and the renormalization scale (MN scheme), the uncertainty of a_γ^{tot} (MX) or a_γ^{tot} (MN) is rather large. Moreover the average value differs from one scheme to the other. In principle, LEC contributions should make low-energy observables independent of the input parameters. In this respect, our results are not quite satisfactory. In the MX scheme, further contributions are definitively required, while in the MN scheme, instead, it appears that an acceptable result could be obtained, provided that a low value of μ is used. Interestingly, this occurs for a value of C_{mn} that roughly compensates the TPEP contribution at short distances, which is partly unphysical. A cancellation on this basis implies $\mu = \Lambda$ in the log term contributing to C_{mn} (and perhaps some modification of the associated constant). Whatever the approach, results show that OPE is a dominant contribution to a_γ , and that the NNLO contributions are in a reasonable range of about 10 ~ 20 % of the OPE contributions for the most stable cases. We would say it reasonable in the sense that the range is obtained with standard values of input parameters and that, at the same time, the amount of the NNLO contribution has the typical size of higher-order corrections in the EFT calculation.

IV. SUMMARY

We have considered the PV NN potential, up to the NNLO, from heavy-baryon chiral-perturbation theory, and applied it to the calculation of the PV asymmetry in $\vec{n}p \rightarrow d\gamma$ at threshold. The OPEP appears at the LO, there is no term at the NLO, and TPEP and CT terms are picked up at the NNLO. Heavy degrees of freedom are integrated out by introducing a monopole form factor in the Fourier transformation of the momentum-space potentials and the corresponding contribution is ascribed to contact terms. A renormalized

LEC is obtained from the dimensional regularization and its form depends on the regularization scheme. We employ the minimal and maximal subtraction schemes to determine this form. Lacking a way to fix the renormalized LEC, we illustrated its contribution by two terms. The first one is obtained from the ρ -resonance saturation of the vector-meson exchange PV potential, and the other one restores the Λ independence of the OPE contribution. In the MN scheme, we have an additional constant term which depends on the renormalization scale. Cutoff dependence is explored with values $\Lambda = 500 \sim 2000$ MeV, and regularization-scheme dependence with renormalization scales $\mu = 2m_\pi \sim 1000$ MeV.

The OPE contribution to the asymmetry is satisfactorily cutoff independent. The TPE potential depends strongly on the cutoff value and is somewhat uncertain, in particular in the intermediate range. As a result, the TPE contribution to the asymmetry varies widely and even shows a change of sign. However, the TPE contribution is bounded by the limiting cutoff value $\Lambda \rightarrow \infty$ and does not exceed about 10% of the OPE one. The LEC contributions are found to be significantly dependent on both the cutoff and renormalization scales introduced in their calculations.

The total sum of OPE, TPE and LEC contributions varies non-negligibly, depending on the choice of the cutoff and renormalization-scale values. With the parameters considered, we have $a_\gamma^{\text{tot}} = -(0.08 \sim 0.11)$. If the PV $\vec{n}p \rightarrow d\gamma$ experiment measures A_γ at the order 10^{-9} , the present result of a_γ^{tot} can fix the first digit of the weak πNN coupling constant h_π^1 unambiguously. However, some caution is needed. In principle, the role of LEC is to account for degrees of freedom whose microscopic description is practically irrelevant for low-energy processes like the one considered here and, at the same time, to make results independent of parameters or regularization schemes employed in their calculation. The present treatment of the LEC doesn't fully satisfy the latter requirement, though some steps in this direction have been considered. Thus, the estimate of a_γ^{tot} made here provides a range in which its *true* value may be, but it is still premature to claim the result for sure. For pinning down the *true* value of a_γ^{tot} , the LEC terms should be treated in a more rigorous and reliable way, *e.g.* fitting them to experimental data if possible, obtaining them with lattice calculations, or making a better use of renormalization group methods. A comparison with earlier TPEP calculations [15, 16, 17] could also be quite useful.

Acknowledgments

The authors would like to thank S.-L. Zhu, C. M. Maekawa, U. van Kolck, M. J. Ramsey-Musolf and B. R. Holstein for useful communications about their published work. We are grateful to H. Fearing for reading the manuscript. We thank the Institute for Nuclear Theory at the University of Washington for its hospitality and the Department of Energy for partial support during the completion of this work. S.A. is supported by Korean Research Foundation and The Korean Federation of Science and Technology Societies Grant funded by Korean Government (MOEHRD, Basic Research Promotion Fund).

-
- [1] S. Weinberg, Phys. Lett. B 251 (1990) 288; Nucl. Phys. B 363 (1991) 3.
 - [2] C. Ordoñez, L. Ray and U. van Kolck, Phys. Rev. C 53 (1996) 2086.
 - [3] E. Epelbaum, W. Glöckle and U.-G. Meißner, Nucl. Phys. A 671 (2000) 295.
 - [4] For a recent review, see, *e.g.*, E. Epelbaum, Prog. Part. Nucl.Phys. 57 (2006) 654, and references therein.
 - [5] C. H. Hyun, T.-S. Park and D.-P. Min, Phys. Lett. B 473 (2000) 6.
 - [6] S.-L. Zhu, C. M. Maekawa, B. R. Holstein, M. J. Ramsey-Musolf and U. van Kolck, Nucl. Phys. A 748 (2005) 435.
 - [7] C. H. Hyun, S. Ando and B. Desplanques, nucl-th/0609015.
 - [8] C.-P. Liu, nucl-th/0609078.
 - [9] B. Desplanques, J. F. Donoghue and B. R. Holstein, Ann. Phys. (N.Y.) 124 (1980) 449.
 - [10] D. B. Kaplan, M. J. Savage, R. P. Springer and M. B. Wise, Phys. Lett. B 449 (1999) 1.
 - [11] B. Desplanques, Phys. Lett. B 512 (2001) 305.
 - [12] C. H. Hyun, T.-S. Park and D.-P. Min, Phys. Lett. B 516 (2001) 321.
 - [13] R. Schiavilla, J. Carlson and M. W. Paris, Phys. Rev. C 70 (2004) 044007; *ibid* 67 (2003) 032501(R).
 - [14] C. H. Hyun, S. J. Lee, J. Haidenbauer and S. W. Hong, Eur. Phys. J. A 24 (2005) 129.
 - [15] B. Desplanques, Phys. Lett. 41B (1972) 461.
 - [16] H. J. Pirner and D. O. Riska, Phys. Lett. B 44 (1973) 151.
 - [17] M. Chemtob and B. Desplanques, Nucl. Phys. B 78 (1974) 139.

[18] B. Desplanques, Nucl. Phys. A 242 (1975) 423.

[19] N. Kaiser and U.-G. Meißner, Nucl. Phys. A 499 (1989) 699.

Hadronic parity violation in $\vec{n}p \rightarrow d\gamma$ with effective field theory

C. H. Hyun,^{1,*} S. Ando,^{1,†} and B. Desplanques^{2,‡}

¹*Department of Physics and Institute of Basic Science,*

Sungkyunkwan University, Suwon 440-746, Korea

²*Laboratoire de Physique Subatomique et de Cosmologie (UMR CNRS/IN2P3-UJF-INPG),*

F-38026 Grenoble Cedex, France

(Dated: November 7, 2006)

Abstract

The parity-violating nucleon-nucleon (NN) potential is considered up to next-to-next-to leading order in heavy-baryon chiral perturbation theory. We include the one-pion exchange at the leading order and the two-pion exchange and two-nucleon contact terms at the next-to-next-to-leading order. The effects of intermediate (two-pion exchange) and short-range (two-nucleon contact) terms are probed by calculating the photon asymmetry A_γ in $\vec{n}p \rightarrow d\gamma$ employing Siegert's theorem and an accurate phenomenological potential for the parity-conserving NN interaction. We explore in detail the uncertainties due to the parameters that control the contribution of the short-range interaction. We obtain about 20% uncertainty in the value of A_γ up to the next-to-next-to leading order. We discuss its implication for the determination of the weak pion-nucleon coupling constant and how the uncertainty can be reduced.

PACS numbers: 21.30.Fe, 12.15.Ji

*Electronic address: hch@meson.skku.ac.kr

†Electronic address: sando@meson.skku.ac.kr

‡Electronic address: desplanq@lpsc.in2p3.fr

I. INTRODUCTION

The perturbative calculation of the strong nucleon-nucleon (NN) potential in the framework of effective-field theory (EFT) was first suggested by Weinberg [1]. Counting rules systematically arrange the magnitude of a two-nucleon irreducible diagram for calculating the NN potential in terms of Q/Λ_χ where Q denotes a typical small momentum and/or pion mass m_π and Λ_χ the chiral scale. Accordingly, one-pion exchange (OPE) and a constant two-nucleon contact term are the most dominant contributions. At the next-to-next-to-leading order (NNLO), there are two-pion exchange (TPE), contact terms with two derivatives and/or pion mass factor, relativistic corrections, *etc.* If one goes to higher orders, there appear multi-pion exchanges and contact terms with more than two derivatives and/or m_π , and heavy-meson exchange possibly comes into play. At low energies where EFT is applicable, a physical process is mostly governed by the long-range interaction and it is more or less insensitive to what's happening in the short-range region. Thus in most cases, heavy mesons are integrated out from the Lagrangian and their short-range interaction is accounted for by contact terms. A physical observable calculated with the NN potential must be independent of a cutoff value that is introduced in calculating loop diagrams and its transformation to coordinate space. This can be achieved by contact terms together with some renormalization method. Strong EFT potentials thus obtained were applied to the analysis of NN scattering phase shifts [2, 3, 4], showing a well-behaved convergence and predictive power. The role of the NNLO potential was intensively explored in [5] where it was shown to be important in extending the predictability of the EFT to higher energies. In addition, its correction to the leading order (LO) potential is non-negligible even at the energy of a few MeV.

The above approach has recently been extended to the parity-violating (PV) nucleon-nucleon (NN) potential [6]. Since then, it has been used for the calculation of observables [7, 8], especially the PV photon asymmetry A_γ in $\vec{n}p \rightarrow d\gamma$ at threshold, where it could be of some relevance.

The PV NN potential is obtained by replacing a parity-conserving (PC) vertex in the strong NN potential with a PV vertex. Most of the low-energy PV calculations have been relying on a one-meson-exchange potential with DDH estimates for the PV meson-nucleon coupling constants [9]. Theoretical estimations of A_γ have been extensively worked out with this model (see Refs. [10, 11, 12, 13, 14] for recent ones). The most elaborate results with

various strong-interaction models [11, 12, 13, 14] turn out to be basically identical. The asymmetry is dominated by the PV one-pion-exchange potential (OPEP) and the heavy-meson contribution is negligible. One can thus discuss whether the measurements of A_γ could provide us with an opportunity to determine the weak pion-nucleon coupling constant h_π^1 . Some literature investigated the PV two-pion-exchange potential (TPEP) in the past [15, 16, 17]. Its contribution to A_γ , calculated with the Hamada-Johnston potential, amounts to about -7% of the OPEP contribution [18]. Not surprisingly, the TPEP is also part of the pionful EFT approach where it appears at NNLO [6]. In the present work, we concentrate on its contribution to the asymmetry A_γ mentioned above and consider the questions that its estimate raises.

Since the PV asymmetry in $\vec{n}p \rightarrow d\gamma$ is sensitive to the one-pion-exchange contribution, we adopt the heavy-baryon chiral perturbation (HB χ PT). We employ the Argonne v18 potential for the PC potential and the Siegert's theorem for the current operators and consider the PV potential relevant to $\vec{n}p \rightarrow d\gamma$ up to NNLO. This calculation will allow us to estimate the order and the magnitude of higher-order corrections, which will be important in pinning down the value of h_π^1 and its uncertainty. At the same time, it will provide a criterion for the validity of the EFT approach to the PV phenomena.

II. FORMALISM

In the HB χ PT, the order of a diagram is counted in terms of a small momentum Q (more precisely Q/Λ_χ) with the following rules; i) a meson propagator is counted as Q^{-2} , ii) a nucleon propagator as Q^{-1} , iii) a loop integral as Q^4 , iv) a vertex as Q^d where d is the number of derivatives at the given vertex. With these counting rules, diagrams in Fig. 1 constitute the contributions up to NNLO. One-pion exchange (a), and the two-pion exchange (b-d) and the contact (CT) (e) terms respectively represent LO and NNLO contributions.

The PV potential is odd in powers of the momentum transfer in momentum space or radial vector in the configuration space, which changes the orbital angular state by an odd number. In order to keep the wave function of a fermion system antisymmetric, the PV potential must satisfy the condition $\Delta(L + S + T) = \text{even}$, where L , S and T denote orbital, spin and isospin states, respectively. The change of $S + T$ in the PV potential should be an odd number. For a two-fermion system, the possible combinations of the spin and isospin

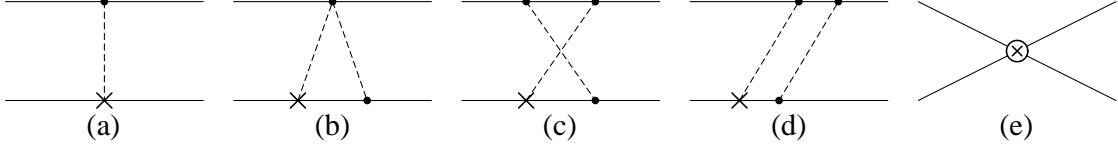


FIG. 1: Diagrams for PV NN potential up to NNLO: (a) for LO ($\mathcal{O}(Q^{-1})$) OPE, and (b-e) for NNLO ($\mathcal{O}(Q^1)$) TPE + CT. Lines (dashed lines) denote nucleons (pions), vertices with a dot represent PC vertices, vertices with “ \times ” represent the PV vertex proportional to h_π^1 , and a vertex with “ \otimes ” denotes the NN contact vertex function proportional to the coefficient C_6^R .

operators in the PV potential must thus be $(\Delta S, \Delta T) = (1, 0)$ or $(0, 1)$. Among various possible combinations of spin and isospin operators that give $\Delta(S + T) = 1$, the term relevant to our estimation of A_γ has the following form in momentum space

$$\tilde{V}_i(\mathbf{q}) = i(\boldsymbol{\tau}_1 \times \boldsymbol{\tau}_2)^z (\boldsymbol{\sigma}_1 + \boldsymbol{\sigma}_2) \cdot \mathbf{q} \tilde{v}_i(q), \quad (1)$$

where $q \equiv |\mathbf{q}|$ and $\mathbf{q} = \mathbf{p}_1 - \mathbf{p}_2$. The OPE, TPE and CT terms are obtained as

$$\tilde{v}_{1\pi}(q) = -\frac{g_A h_\pi^1}{2\sqrt{2}f_\pi} \frac{1}{q^2 + m_\pi^2}, \quad (2)$$

$$\tilde{v}_{2\pi}(q) = \sqrt{2}\pi \frac{h_\pi^1}{\Lambda_\chi^3} \left\{ g_A \tilde{L}(q) - g_A^3 [3\tilde{L}(q) - \tilde{H}(q)] \right\}, \quad (3)$$

$$\tilde{v}_{\text{CT}} = C_6^R, \quad (4)$$

with

$$\tilde{L}(q) = \frac{\sqrt{q^2 + 4m_\pi^2}}{q} \ln \left(\frac{\sqrt{q^2 + 4m_\pi^2} + q}{2m_\pi} \right), \quad (5)$$

$$\tilde{H}(q) = \frac{4m_\pi^2}{q^2 + 4m_\pi^2} \tilde{L}(q), \quad (6)$$

where g_A is the axial coupling constant, f_π the pion-decay constant and $\Lambda_\chi = 4\pi f_\pi$. The constant C_6^R is the renormalized LEC for a NN contact term C_6 in [6]. It subsumes the role of all the heavy degrees of freedom integrated out from the theory. We will discuss how to treat the renormalized LEC in our investigation after giving the formulae of the potentials in configuration space.

The potential in Eq. (1) transformed to the configuration space takes the form

$$\begin{aligned} V_i(\mathbf{r}) &= \int \frac{d^3\mathbf{q}}{(2\pi)^3} \tilde{V}_i(\mathbf{q}) e^{-i\mathbf{q}\cdot\mathbf{r}} \\ &= i(\boldsymbol{\tau}_1 \times \boldsymbol{\tau}_2)^z (\boldsymbol{\sigma}_1 + \boldsymbol{\sigma}_2) \cdot [\mathbf{p}, v_i(r)], \end{aligned} \quad (7)$$

where \mathbf{p} is the conjugate momentum of the relative coordinate $\mathbf{r} \equiv \mathbf{r}_1 - \mathbf{r}_2$. For an easier numerical calculation, we rewrite Eqs. (5, 6) into the dispersion-relation form as

$$\tilde{L}(q) = - \int_{4m_\pi^2}^{\infty} \frac{dt'}{2\sqrt{t'}} \sqrt{t' - 4m_\pi^2} \left(\frac{1}{t' + q^2} - \frac{1}{t' - 4m_\pi^2} \right), \quad (8)$$

$$\tilde{H}(q) = \frac{4m_\pi^2}{2} \int_{4m_\pi^2}^{\infty} \frac{dt'}{\sqrt{t'}} \frac{1}{\sqrt{t' - 4m_\pi^2}} \frac{1}{t' + q^2}. \quad (9)$$

In calculating the Fourier transformation of Eq. (1) and in order to make it analytically, we introduce monopole form factors of the type $(\Lambda^2 - m_\pi^2)/(\Lambda^2 + q^2)$ in Eq. (2) and $\Lambda^2/(\Lambda^2 + q^2)$ in Eqs. (3, 4). The particular choice for the OPEP preserves the long-range part, which, otherwise, could not be easily corrected for with contact interactions. The roles of the form factor and the cutoff are (i) to make the numerical calculation easier and more efficient, and (ii) to cut away the high-momentum region where the dynamics is essentially unknown and whose detail is irrelevant to low-energy processes. It is reminded that the cutoff is arbitrary for a part and that final results should not depend on its value. With the form factor, we rewrite the potential in configuration space as

$$V_i^\Lambda(\mathbf{r}) = i(\boldsymbol{\tau}_1 \times \boldsymbol{\tau}_2)^z (\boldsymbol{\sigma}_1 + \boldsymbol{\sigma}_2) \cdot [\mathbf{p}, v_i^\Lambda(r)], \quad (10)$$

where

$$v_{1\pi}^\Lambda(r) = \frac{g_A h_\pi^1}{2\sqrt{2}f_\pi} \frac{1}{4\pi r} (e^{-m_\pi r} - e^{-\Lambda r}), \quad (11)$$

$$v_{2\pi}^\Lambda(r) = \sqrt{2}\pi \frac{h_\pi^1}{\Lambda_\chi^3} \left\{ g_A L^\Lambda(r) - g_A^3 [3L^\Lambda(r) - H^\Lambda(r)] \right\}, \quad (12)$$

$$v_{\text{CT}}^\Lambda(r) = -C_6^R \Lambda^2 \frac{e^{-\Lambda r}}{4\pi r}, \quad (13)$$

with

$$L^\Lambda(r) = \frac{\Lambda^2}{8\pi r} \int_{4m_\pi^2}^{\infty} \frac{dt'}{\sqrt{t'}} \sqrt{t' - 4m_\pi^2} \left(\frac{e^{-\sqrt{t'}r} - e^{-\Lambda r}}{\Lambda^2 - t'} - \frac{e^{-\Lambda r}}{t' - 4m_\pi^2} \right), \quad (14)$$

$$H^\Lambda(r) = -\frac{m_\pi^2 \Lambda^2}{2\pi r} \int_{4m_\pi^2}^{\infty} \frac{dt'}{\sqrt{t'}} \frac{1}{\sqrt{t' - 4m_\pi^2}} \frac{e^{-\sqrt{t'}r} - e^{-\Lambda r}}{\Lambda^2 - t'}. \quad (15)$$

Notice that in the $\Lambda \rightarrow \infty$ limit, $L^\Lambda(r)$ is the difference of terms as singular as r^{-3} and $\delta(\vec{r})$ with an infinite coefficient. The 3-dimensional integral over \vec{r} is however finite and has the sign of the contact term.

The form of C_6^R depends on the regularization scheme. In Ref. [6], all the constant terms obtained from the dimensional regularization ($d = 4 - 2\epsilon$) of TPE diagrams are included in C_6^R , leading to

$$C_6^R(\text{MX}) = C_6 - h_\pi^1 \frac{\pi g_A}{\sqrt{2} \Lambda_\chi^3} (1 - 3g_A^2) \left[\frac{1}{\epsilon} - \gamma + \ln(4\pi) + 2 \ln \left(\frac{\mu}{m_\pi} \right) + 2 \right], \quad (16)$$

where the abbreviation MX stands for ‘maximal subtraction’, $\gamma = 0.5772$ and μ is the renormalization scale. In the minimal subtraction (MN in short), the renormalized LEC satisfies the relation

$$C_6^R(\text{MX}) = C_6^R(\text{MN}) + C_{\text{mn}}, \quad (17)$$

where

$$C_{\text{mn}} = -h_\pi^1 \frac{\sqrt{2} \pi g_A}{\Lambda_\chi^3} (1 - 3g_A^2) \left[\ln \left(\frac{\mu}{m_\pi} \right) + 1 \right]. \quad (18)$$

Either $C_6^R(\text{MX})$ or $C_6^R(\text{MN})$ has to be determined from the calculation with the underlying theory or experimental data with good statistics but none of them is available at present. We can only consider possible contributions to C_6^R , leaving for the future the theoretical or experimental determination of the remaining part.

A first contribution is suggested by the one-meson exchange model. In the heavy-meson limit, the leading order of the ρ -meson propagator is a constant and the corresponding term can be regarded as part of C_6^R . It reads

$$C_6^R(\rho) = \frac{g_{\rho NN} h_\rho^{1'}}{2m_N m_\rho^2}, \quad (19)$$

where $h_\rho^{1'}$ is a PV ρNN coupling constant in the potential. A non-vanishing value is obtained for this coupling in a soliton model, $h_\rho^{1'} = -2.2 \times 10^{-7}$ [19]. Leaving aside consistency problems between different approaches, double counting with TPEP considered here for instance, we notice that it compares to the DDH best value of h_π^1 ($= 4.6 \times 10^{-7}$). The corresponding value of $C_6^R(\rho)$ is $-1.20 \times 10^{-9} \text{ MeV}^{-3}$ in unit of this value of h_π^1 .

A second contribution is provided by the MN scheme where C_{mn} is treated independently of $C_6^R(\text{MN})$, which consequently gives μ dependence in the result. If we choose $\mu = m_\rho$, we have $C_{\text{mn}} = 4.174 \times 10^{-8} \text{ MeV}^{-3}$ in unit of h_π^1 . This value is one order larger than $C_6^R(\rho)$, and therefore the effect of C_{mn} and the dependence on μ can be non-negligible.

A third contribution stems from a deeper examination of the TPEP. This one has been obtained by removing from the square-box diagram the iterated OPEP, ignoring the cutoff

introduced in actual calculations. The correction, which involves the whole strong interaction and should contribute to make the results cutoff independent, is not easy to calculate. This last property can however be restored with a minimal contribution which cancels the cutoff-dependent term in Eq. (11). This one corresponds to

$$C_6^R(\pi, \Lambda) = -\frac{g_A h_\pi^1}{2\sqrt{2}f_\pi\Lambda^2}. \quad (20)$$

Its value compares to the C_{mn} one for the smallest values of the cutoff Λ considered here.

We will explore the above contributions in detail in the analysis of the photon asymmetry in $\vec{n}p \rightarrow d\gamma$, A_γ . This one is defined from the differential cross section of the process as

$$\frac{d\sigma}{d\Omega} \propto 1 + A_\gamma \cos \theta, \quad (21)$$

where θ is the angle between the neutron polarization and the out-going photon momentum. Non-zero A_γ values arise from the interference of opposite-parity transition amplitudes, *e.g.* M1 and E1. At the thermal energy where the process occurs, lowest order EM operators may suffice, therefore we consider the E1 operator,

$$\mathbf{J}_{\text{E1}} = -i\frac{\omega_\gamma}{4} (\tau_1^z - \tau_2^z) \mathbf{r}, \quad (22)$$

where ω_γ is the out-going-photon energy. At the leading order of h_π^1 , A_γ is proportional to h_π^1 , and we can write A_γ as

$$A_\gamma = a_\gamma h_\pi^1, \quad (23)$$

with

$$a_\gamma = -2\frac{\text{Re}(\mathcal{M}_1\mathcal{E}_1^*)}{|\mathcal{M}_1|^2}, \quad (24)$$

where \mathcal{E}_1 and \mathcal{M}_1 are matrix elements of the E1 and M1 transitions, respectively. Analytic forms of these amplitudes can be found in [14].

III. RESULTS AND DISCUSSION

We here present and discuss numerical results corresponding to various contributions outlined in the previous section. The OPE and TPE potentials in configuration space are considered as well as individual and total contributions to the A_γ asymmetry.

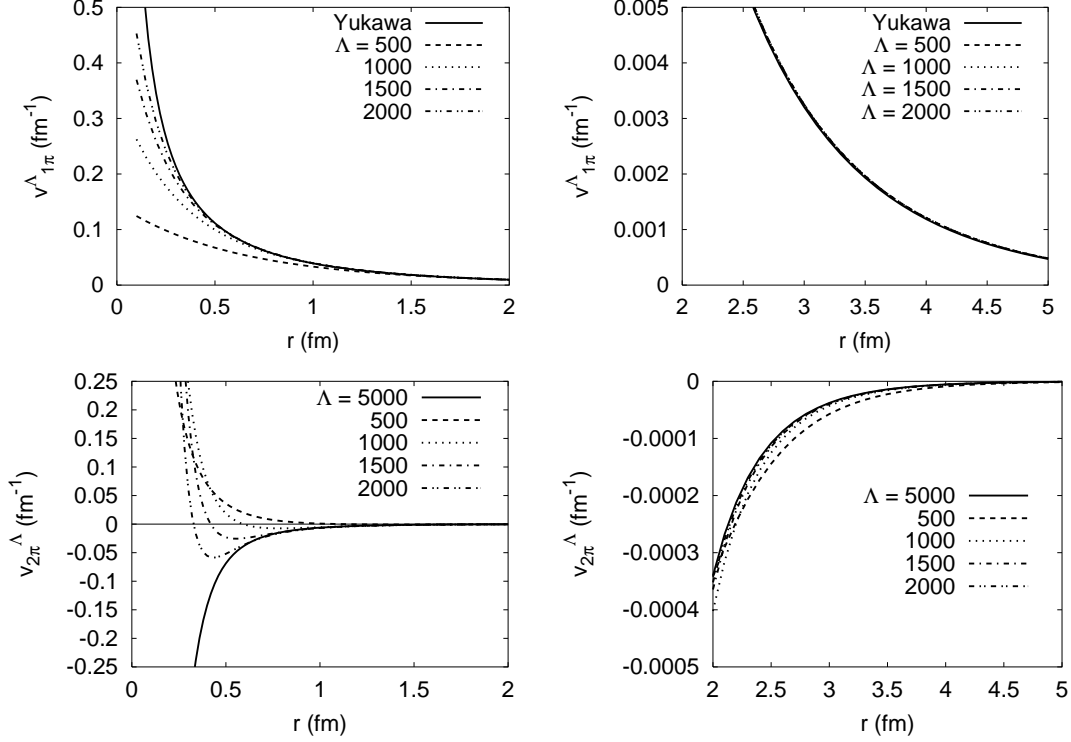


FIG. 2: Potentials $v_{1\pi}^\Lambda(r)$ (upper row) and $v_{2\pi}^\Lambda(r)$ (lower row) divided by h_π^1 in the short-intermediate (left column) and long (right column) ranges. In the figures for TPEP, the result of $\Lambda = 5000$ MeV is shown as an example of the limiting case $\Lambda \rightarrow \infty$.

The OPEP term $v_{1\pi}^\Lambda(r)$ is shown in the top rows of Fig. 2 in the short (left) and long (right) ranges separately. The curve denoted by ‘Yukawa’ corresponds to the infinite-cutoff value. Increasing the cutoff Λ , the potential converges to the Yukawa one. It is almost independent of the cutoff value in the range $r > 1$ fm and deviates from the others at $r < 1$ fm with a cutoff of 500 MeV, and at roughly $r = 0.5$ fm with a cutoff of 1000 MeV.

The TPEP term $v_{2\pi}^\Lambda(r)$ is in the bottom rows of Fig. 2. The long-range behavior is, as OPEP, independent of the cutoff value, but its magnitude is smaller by an order of magnitude. Therefore one can conclude that the long-range dynamics is essentially cutoff independent and governed by OPEP. On the contrary, TPEP changes sign in the intermediate or short range (bottom-left panel), and the position at which the sign change occurs depends on the cutoff value. What matters in this behavior is that this change occurs in the intermediate region where TPEP is supposed to play an important role. The effect of this strong cutoff dependence is investigated below for the physical observable of interest here.

Λ (MeV)	500	1000	1500	2000
a_γ^{OPE}	-0.0992	-0.1104	-0.1117	-0.1119
a_γ^{TPE}	-0.0022	0.0073	0.0117	0.0133
$a_\gamma^{\text{LEC}}(\rho)$	-0.0008	-0.0004	-0.0002	-0.0001
$a_\gamma^{\text{LEC}}(\text{mn})$	0.0264	0.0134	0.0065	0.0036
$a_\gamma^{\text{LEC}}(\pi, \Lambda)$	-0.0128	-0.0016	-0.0004	-0.0001

TABLE I: Contribution to the asymmetry from each term as a function of the cutoff Λ . The renormalization scale is chosen as $\mu = m_\rho$ in the minimal subtraction LEC contribution ($\propto C_{\text{mn}}$).

Table I shows the contribution of each term to the coefficient a_γ entering the expression of the asymmetry A_γ , Eq. (23). The OPEP contribution with $\Lambda = 500$ MeV is slightly smaller in magnitude than those with the other cutoff values, but the result as a whole is independent of the cutoff value. The small difference of a_γ^{OPE} with $\Lambda = 500$ MeV can be attributed to the deviation of $v_{1\pi}^\Lambda(r)$ in the range $r < 1$ fm with $\Lambda = 500$ MeV from those with the other cutoff values. On the other hand, it seems that the region below $r \sim 0.5$ fm gives an almost negligible contribution since $v_{1\pi}^\Lambda(r)$ with $\Lambda = 1000$ MeV differs sizably from those with larger cutoff values below $r \sim 0.5$ fm, but the difference for a_γ^{OPE} is negligible. Roughly speaking, the significant contribution to a_γ comes from the region $r \gtrsim 0.5$ fm.

The TPEP contribution to a_γ , on the other hand, varies significantly in sign and magnitude. The change of a_γ^{TPE} can be attributed to the strong dependence of $v_{2\pi}^\Lambda(r)$ on the cutoff value in the intermediate and short ranges. The sign change, which can be ascribed to a contact term implied by the method used to calculate the potential, is physically questionable. From the behavior of $v_{1\pi}^\Lambda(r)$ and the sign of a_γ^{OPE} , one can deduce that a decreasing term gives a negative contribution to a_γ . With a smaller cutoff value, the decreasing part of TPEP spreads to a larger r . For instance, TPEP becomes increasing at around $r = 0.4$ fm for $\Lambda = 2000$ MeV, but this occurs around 1.5 fm for $\Lambda = 500$ MeV. In the discussion of a_γ^{OPE} , we argued that most of the contribution arises from the region $r \gtrsim 0.5$ fm. With a smaller cutoff value, the negative contribution to a_γ^{TPE} becomes more substantial and, as a result, a_γ^{TPE} with $\Lambda = 500$ MeV is negative. The convergence of the TPE contribution with an increasing cutoff value is slower than the OPE one, which can also be attributed to the

Λ (MeV)	500	1000	1500	2000
$a_\gamma^{\text{tot}}(\text{MX})$	-0.1149	-0.1051	-0.1006	-0.0988
	-0.0987	-0.0969	-0.0966	-0.0966
$a_\gamma^{\text{tot}}(\text{MN})$	-0.0885	-0.0917	-0.0941	-0.0952
	-0.0859	-0.0904	-0.0935	-0.0949

TABLE II: Total sum of OPE, TPE and LEC contributions in the MX and MN schemes. Each row of $a_\gamma^{\text{tot}}(\text{MN})$ corresponds to $\mu = 2m_\pi$, m_ρ and 1000 MeV from the top, respectively.

strong dependence of TPEP on the cutoff value. However, a_γ^{TPE} will not increase indefinitely and we guess that a_γ^{TPE} with $\Lambda = 2000$ MeV will not be much different from that in the limiting case $\Lambda \rightarrow \infty$. For example, $a_\gamma^{\text{TPE}} = 0.0146$ with $\Lambda = 5000$ MeV, whose increase rate with respect to Λ is very lowered down compared to that in the smaller Λ region. Thus, without significant error, we can conclude that the TPE contribution to a_γ is about 10% of the OPE.

All the LEC contributions ($\propto C_6^R(\rho)$, C_{mn} and $C_6^R(\pi, \Lambda)$) have a magnitude that decreases with increasing cutoff value. With a smaller cutoff value, $v_{\text{CT}}^\Lambda(r)$ is less short-range peaked and spreads broader to larger r . Reminding the $r \gtrsim 0.5$ fm criterion, it is a natural result to have a a_γ^{LEC} smaller in magnitude with a larger cutoff. It is noticed that the $C_6^R(\rho)$ contribution is small in comparison of the other ones but this could be a result of the particular value of $h_\rho^{1'}$ used in its calculation [19]. The contribution of the C_{mn} term, absent in the MX scheme, compares to the TPEP one. Consequently, the choice of the regularization scheme can give a non-trivial effect for the total sum of OPE, TPE and LEC contributions, a_γ^{tot} . The $C_6^R(\pi, \Lambda)$ contribution also compares to the TPEP one, but only at small Λ . As expected from its derivation, it removes the Λ dependence of the OPE contribution.

In Table II, we show the sum of OPE, TPE and LEC contributions to a_γ , for the MX and MN regularization schemes. Columns give insight on the cutoff dependence while rows in the MN case show how results vary with the renormalization scale, μ . This one is conventionally set to the ρ -meson mass, the chiral symmetry breaking scale Λ_χ or also the order of the cutoff value Λ [4]. Exploring the corresponding dependence with values $\mu = 2m_\pi$, m_ρ and 1000 MeV, a_γ^{tot} is found to increase with μ (algebraically). This is simply related to the contribution of the C_{mn} term which is a logarithmically increasing function of that

variable. Concerning the dependence on the cutoff value, it is found to be opposite in the MX scheme and the MN one with $\mu = m_\rho$. As the OPE together with the $C_6^R(\pi, \Lambda)$ and $C_6^R(\rho)$ contributions remains almost constant, the Λ dependence in the MX scheme is mainly due to the TPE one. The opposite effect in the MN scheme results from the further LEC contribution involving C_{mn} , which roughly has the same magnitude but is decreasing instead of increasing with Λ . It is noticed that the overall Λ dependence is sensitive to the μ value and can almost vanish ($\mu = 2m_\pi$) as well as be more pronounced ($\mu = 1000$ MeV).

Because of the considerable dependence on the cutoff Λ (MX scheme) or on both the cutoff and the renormalization scale (MN scheme), the uncertainty of a_γ^{tot} (MX) or a_γ^{tot} (MN) is rather large. Moreover the average value differs from one scheme to the other. In principle, LEC contributions should make low-energy observables independent of the input parameters. In this respect, our results are not quite satisfactory. In the MX scheme, further contributions are definitively required, while in the MN scheme, instead, it sounds that an acceptable result could be obtained, provided that a low value of μ is used. Interestingly, this occurs for a value of C_{mn} that roughly compensates the TPEP contribution at short distances, which is partly unphysical. A cancellation on this basis implies $\mu = \Lambda$ in the log term contributing to C_{mn} (and perhaps some modification of the associated constant). Whatever the approach, results show that OPE is a dominant contribution to a_γ , and that the NNLO contributions are in a reasonable range of about $10 \sim 20$ % of the OPE one for the most stable cases. We would say it reasonable in the sense that the range is obtained with standard values of input parameters and that, at the same time, the amount of the NNLO contribution has the typical size of higher-order corrections in the EFT calculation.

IV. SUMMARY

We have considered the PV NN potential up to the NNLO from the heavy-baryon chiral-perturbation theory, and applied it to the calculation of the PV asymmetry in $\vec{n}p \rightarrow d\gamma$ at threshold. The OPEP appears at the LO, there is no term at the NLO, and TPEP and CT terms are picked up at the NNLO. Heavy degrees of freedom are integrated out by introducing a monopole form factor in the Fourier transformation of the momentum-space potentials and the corresponding contribution is ascribed to contact terms. A renormalized LEC is obtained from the dimensional regularization and its form depends on the regulari-

zation scheme. We employ the minimal and maximal subtraction schemes to determine this form. Lacking a way to fix the renormalized LEC, we illustrated its contribution, for a part, with a constant obtained from the ρ -resonance saturation of the vector-meson exchange PV potential. Another part restores the Λ independence of the OPE contribution. In the MN scheme, we have an additional constant term which depends on the renormalization scale. Cutoff dependence is explored with values $\Lambda = 500 \sim 2000$ MeV, and regularization-scheme dependence with renormalization scales $\mu = 2m_\pi \sim 1000$ MeV.

The OPE contribution to the asymmetry is satisfactorily cutoff independent. The TPE potential depends strongly on the cutoff value and is somewhat uncertain, in particular in the intermediate range. As a result, the TPE contribution to the asymmetry varies widely and even shows a change of sign. However, the TPE contribution is bounded by the limiting cutoff value $\Lambda \rightarrow \infty$ and does not exceed about 10% of the OPE one. The LEC contributions are found to be significantly dependent on both the cutoff and renormalization scale introduced in their calculations.

The total sum of OPE, TPE and LEC contributions varies non-negligibly, depending on the choice of the cutoff and renormalization-scale values. With the considered parameters, we have $a_\gamma^{\text{tot}} = -(0.08 \sim 0.11)$. If the PV $\vec{n}p \rightarrow d\gamma$ experiment measures A_γ at the order 10^{-9} , the present result of a_γ^{tot} can fix the first digit of the weak πNN coupling constant h_π^1 unambiguously. However, some caution is needed. In principle, the role of LEC is to account for degrees of freedom whose microscopic description is practically irrelevant for low-energy processes like the one considered here and, at the same time, to make results independent of parameters or regularization schemes employed in their calculation. The present treatment of the LEC doesn't fully satisfy the latter requirement, though some steps in this direction have been considered. Thus, the estimate of a_γ^{tot} made here provides a range in which its *true* value may be, but it is still premature to claim the result for sure. For pinning down the *true* value of a_γ^{tot} , the LEC terms should be treated in a more rigorous and reliable way, *e.g.* fitting them to experimental data if possible, obtaining them with lattice calculations, or making a better use of renormalization group methods. A comparison with earlier TPEP calculations [15, 16, 17] could also be quite useful.

Acknowledgments

The authors would like to thank S.-L. Zhu, C. M. Maekawa, U. van Kolck, M. J. Ramsey-Musolf and B. R. Holstein for useful communications about their published work. S.A. is supported by Korean Research Foundation and The Korean Federation of Science and Technology Societies Grant funded by Korean Government (MOEHRD, Basic Research Promotion Fund).

-
- [1] S. Weinberg, Phys. Lett. B 251 (1990) 288; Nucl. Phys. B 363 (1991) 3.
 - [2] C. Ordoñez, L. Ray and U. van Kolck, Phys. Rev. C 53 (1996) 2086.
 - [3] E. Epelbaum, W. Glöckle and U.-G. Meißner, Nucl. Phys. A 671 (2000) 295.
 - [4] For a recent review, see, *e.g.*, E. Epelbaum, Prog. Part. Nucl.Phys. 57 (2006) 654, and references therein.
 - [5] C. H. Hyun, T.-S. Park and D.-P. Min, Phys. Lett. B 473 (2000) 6.
 - [6] S.-L. Zhu, C. M. Maekawa, B. R. Holstein, M. J. Ramsey-Musolf and U. van Kolck, Nucl. Phys. A 748 (2005) 435.
 - [7] C. H. Hyun, S. Ando and B. Desplanques, nucl-th/0609015.
 - [8] C.-P. Liu, nucl-th/0609078.
 - [9] B. Desplanques, J. F. Donoghue and B. R. Holstein, Ann. Phys. (N.Y.) 124 (1980) 449.
 - [10] D. B. Kaplan, M. J. Savage, R. P. Springer and M. B. Wise, Phys. Lett. B 449 (1999) 1.
 - [11] B. Desplanques, Phys. Lett. B 512 (2001) 305.
 - [12] C. H. Hyun, T.-S. Park and D.-P. Min, Phys. Lett. B 516 (2001) 321.
 - [13] R. Schiavilla, J. Carlson and M. W. Paris, Phys. Rev. C 70 (2004) 044007; *ibid* 67 (2003) 032501(R).
 - [14] C. H. Hyun, S. J. Lee, J. Haidenbauer and S. W. Hong, Eur. Phys. J. A 24 (2005) 129.
 - [15] B. Desplanques, Phys. Lett. 41B (1972) 461.
 - [16] H. J. Pirner and D. O. Riska, Phys. Lett. B 44 (1973) 151.
 - [17] M. Chemtob and B. Desplanques, Nucl. Phys. B 78 (1974) 139.
 - [18] B. Desplanques, Nucl. Phys. A 242 (1975) 423.
 - [19] N. Kaiser and U.-G. Meißner, Nucl. Phys. A 499 (1989) 699.